Otx2 signals from the choroid plexus to regulate adult neurogenesis

Anabelle Planques[1], Vanessa Oliveira Moreira[1], Chantal Dubreuil, Alain Prochiantz, Ariel A Di Nardo[*]

Centre for Interdisciplinary Research in Biology (CIRB), Collège de France, CNRS UMR 7241, INSERM U1050, PSL Research University, Paris, France.

[1]co-first authors
[*]corresponding author: ariel.dinardo@college-de-france.fr

Abstract
Proliferation and migration during adult neurogenesis are regulated by a microenvironment originating from local vasculature, from cerebrospinal fluid produced by the choroid plexus, and from local supporting cells including astrocytes. Here, we focus on the function of Otx2 homeoprotein transcription factor in the adult subventricular zone which generates olfactory bulb neurons. We find that Otx2 secreted by choroid plexus is transferred to supporting cells of the subventricular zone and rostral migratory stream. Deletion of *Otx2* in choroid plexus reduces the number of olfactory bulb newborn neurons and modifies extracellular matrix components produced by astrocytes. By expressing secreted single-chain antibodies to sequester Otx2 in the cerebrospinal fluid, we obtain similar results, demonstrating the importance of non-cell autonomous Otx2 in adult neurogenesis and suggesting a pivotal role for astrocytes. By using *in vitro* astrocytes co-cultured with neurospheres, we show that Otx2 down-regulates tenascin-C expression and subsequently modifies neuroblast migration. Thus, we reveal a multi-level and non-cell autonomous role of a homeoprotein, and reinforce the idea of the choroid plexus as a key niche compartment affecting adult neurogenesis.

Introduction

Neurogenesis in the adult mouse brain provides continuous replacement of interneurons in olfactory bulbs (OB) and is important for olfaction-based learning[1]. Neural stem cells, located in the adult subventricular zone (aSVZ) lining the lateral cerebral ventricles, give rise to progenitor cells (neuroblasts) that migrate though the rostral migratory stream (RMS) to reach the OB where they differentiate as interneurons and integrate into the network. The RMS is composed of a compacted neuroblast network forming chains that migrate along blood vessels and are surrounded by astrocytic processes[2,3]. While it is clear that RMS-associated astrocytes interact with neuroblasts[4], the role of astrocytes for neuroblast migration is not well known. Astrocytes are also located in the aSVZ and are thought to play a role as supporting cells for regulating the neurogenic niche microenvironment[5]. The niche is further influenced by extrinsic factors coming from local vasculature and the cerebrospinal fluid (CSF)[6]. Furthermore, neural stem cells interact directly with both vasculature and CSF[7]. Indeed, it has been shown that molecules within the CSF can control aSVZ neurogenesis by regulating cell proliferation[8] or migration[9].

Homeoproteins are key regulators of neurogenesis both during embryogenesis and adult neurogenesis[10,11]. This class of transcription factors have the property to act both cell-autonomously and non-cell-autonomously after secretion and internalization in target cells. The Otx2 homeoprotein is expressed by choroid plexus (CP), secreted in CSF, and transfers in brain parenchyma to regulate visual cortex plasticity in postnatal mice[12]. Otx2 is a regulator of embryonic development and embryonic neurogenesis[13] but its role on adult neurogenesis has not been investigated. We show that Otx2 transfers in supporting cells of aSVZ-RMS neurogenic niche and impacts neurogenesis by modifying the expression of astrocyte-derived extracellular matrix (ECM).

Results

Otx2 knockdown in choroid plexus leads to reduced integration of newborn neurons in the olfactory bulb

In the adult mouse, continuous production of aSVZ progenitors and integration of new neurons in the OB are regulated in part by factors coming from the CSF[6,7]. Given that Otx2 is expressed and secreted by CP, we first examined whether *Otx2* knockdown in CP alters aSVZ neurogenesis. We have previously shown that Cre-Tat intracerebroventricular injections in lateral ventricles of *Otx2*$^{lox/lox}$ (Otx2-lox) mice lead to specific recombination of *Otx2* gene in CP[12]. We now extend this result by confirming that this paradigm leads not only to a strong decrease of *Otx2* expression in lateral ventricle CP (41.1% ± 14.3 SD of *Otx2* expression compared to vehicle-injected mice, Fig. 1a,b), but also to a directly proportional decrease of *Otx2* mRNA in both lateral and 4th ventricle CP (Fig. 1c, p=0.0007). This allows for the use of 4th ventricle CP to assess *Otx2* expression levels while anterior tissues are used for histology. Cre-Tat-injected animals with less than 30% *Otx2* expression knockdown were removed from analysis.

Different BrdU injection paradigms were used to evaluate aSVZ neurogenesis. A first paradigm quantified BrdU+ cells in OB three weeks after BrdU injections to evaluate newborn neuron integration in OB (Fig. 1d). A second paradigm quantified BrdU+ cells in aSVZ 2 hours after BrdU injection to evaluate progenitor cell proliferation (Fig. 1j). In the first paradigm, significantly fewer BrdU+ cells were counted in granule cell layer (GCL) of Cre-Tat-injected mice compare to vehicle-injected mice (75.6% ± 21.3 SD of vehicle, Fig. 1e, f) while there was no change in glomerular layer (GL) (92.2% ± 22.8 SD of vehicle, Fig. 1e, g). Analysis of Caspase-expressing cells revealed no change in cell death in the RMS of Cre-Tat-injected mice (89,9% ± 31.2 SD of vehicle, Fig. 1h,i), nor in the OB (data not shown),

suggesting that Otx2 does not affect neuroblast survival. In the second paradigm, Cre-Tat-injected mice showed similar cell proliferation in aSVZ (98.6% ± 13.7 SD of vehicle, Fig. 1k,l). Therefore, *Otx2* expression in CP regulates aSVZ neurogenesis, although the reduced number of newborn neuron integration in GCL is not a consequence of reduced aSVZ proliferation.

Non-cell-autonomous Otx2 in aSVZ and RMS

Given that *Otx2* expression in CP impacts aSVZ neurogenesis and is able to transfer in brain parenchyma[12] we hypothesized that Otx2 transfers from CP to the aSVZ niche. The *Otx2* locus is silent in aSVZ and RMS, as shown by the absence of GFP expression in $Otx2^{+/GFP}$ mice (Fig. 2a,b) and by *in situ* hybridization (Fig. 2c). However, we were able to immunoprecipitate Otx2 protein from lysates of aSVZ and RMS microdissections (Fig. 2d,e), as confirmed by lysates of superior colliculus as positive control and of striatum (microdissected beneath aSVZ) as negative control (Fig. 2e). Immunostaining showed selective presence of Otx2 in a subset of cells within the aSVZ, RMS and OB (Fig. 2f-h).

Given the presence of Otx2 protein in these neurogenic niches, the correlation between neurogenesis and choroid plexus *Otx2* expression could be due to Otx2 non-cell-autonomous activity. To address this possibility specifically, we used a single chain antibody (scFv) mouse model (scFv-Otx2 mice) that sequesters Otx2 in the CSF and blocks its transfer[14]. Intracerebroventricular injections of Cre-Tat lead to local scFv-Otx2 expression by CP cells (GFP reporter, Fig. 3a) and secretion into the CSF[14]. Subjecting these mice to the BrdU paradigm for OB integration (Fig. 1d) revealed a decrease in newborn neurons in the GCL of Cre-Tat-injected animals (71.7% ± 17.8 SD of vehicle, Fig. 3b) and no significant change in the GL (82.9% ± 14.7 SD of vehicle, Fig. 3c). This decrease is similar to what was observed in the CP *Otx2* knockdown model (Fig. 1f,g), and suggests that Otx2 transfer from CSF to aSVZ plays a significant role in regulating adult neurogenesis.

Given that Otx2 is transferring to a subset of aSVZ and RMS cells (Fig. 2), it could be targeting either neural stem cells or progenitor cells directly and/or other cells within the niche. Immunostaining revealed that Otx2 is not internalized in neuroblasts in aSVZ (Fig. 4a) and RMS (Fig. 4c). Indeed, we find Otx2 in GFAP-labeled cells and ependymal cells of aSVZ (Fig. 4a,b). In RMS, Otx2 was also found in GFAP labeled cells (Fig. 4c,d). The accumulation of Otx2 protein in supporting cells within the niche suggests that Otx2 regulates aSVZ neurogenesis though modification of the niche microenvironment.

Otx2 regulates ECM and neuroblast migration

In aSVZ and RMS, Thrombospondin-4 (Thbs4) and Tenascin-C (Tnc) are ECM proteins expressed by astrocytes[15,16]. We found that both *Thbs4* and *Tnc* were upregulated in aSVZ of Cre-Tat injected Otx2-lox mice (304.6% ± 114.5 SD and 201.1% ± 94 SD of vehicle respectively, Fig. 5a,b) and of Cre-Tat injected scFv-Otx2 mice (Fig 5c,d)). This suggests that Otx2 transfers to niche astrocytes and regulates neurogenesis by controlling ECM composition. To further investigate Otx2 regulation of astrocytes, we used an *in vitro* paradigm consisting of adult neurospheres plated on a bed of astrocytes (Fig. 5e). Treatment with Otx2 protein or transfection with Otx2 plasmid leads to reduced Tnc expression in astrocytes (Fig. 5f). When neurospheres are plated on astrocytes that express Otx2, we observed significant increase in neuroblast migration (Fig 5i). Therefore, the effects of Otx2 gain-of-function *in vitro* is consistent with *in vivo* knockdown experiments: negative regulation of Tnc by Otx2.

Discussion

Through specific conditional recombination in the choroid plexus of two mouse models, similar decreases in neurogenesis were observed. With the Otx2-lox mice, recombination results in loss of local Otx2 expression in the choroid plexus, while with the scFv-Otx2 mice it results in sequestering Otx2 in the CSF. The first model includes both potential cell-autonomous effects of loss of Otx2 in the choroid plexus as well potential non-cell-autonomous effects through reduced levels of secreted Otx2. The second model comprises only non-cell-autonomous effects as only secreted Otx2 is affected. This is confirmed by the absence of autocrine effects (i.e. CSF Otx2 signaling on choroid plexus) assessed by choroid plexus mRNA levels of Otx2 transcription targets upon scFv expression[14]. Since both models provide a similar reduction in the number of newborn neurons, it suggests that Otx2 non-cell-autonomous function is of primary importance for adult neurogenesis.

The specific internalization of Otx2 in aSVZ and RMS astrocytes might be a consequence of specialized ECM around these cells. In the visual cortex, Otx2 is specifically internalized by parvalbumin interneurons, which have a unique and stable ECM called perineuronal nets (PNN) that often stain for the lectin *Wisteria floribunda* (WFA)[17]. The specificity of internalization arises from a glycosaminoglycan-binding motif in Otx2 protein[18,19]. However, staining for WFA is not detected in the aSVZ, which is not surprising given that PNN are synonymous with consolidation of ECM and a break on plasticity – events that would counter the function of the neurogenic niche. Although specific target glycosaminoglycans of Otx2 have yet to be identified, the hypothesis of ECM-Otx2 interaction accounting for the specific internalization remains the most plausible, given that homeoprotein cell-surface receptors have not been found[20].

Neurogenesis is impacted by the composition of ECM in stem cells niches[21]. ECM glycoproteins and proteoglycans can trap molecules that signal through receptors or through direct internalization. Astrocytes in the aSVZ and RMS secrete many ECM molecules including Tnc and Thbs4[16,22,23]. Thbs4 is expressed only by astrocytes specifically in the aSVZ and RMS[15,24], while Tnc is also expressed in other regions of the brain. *Thbs4* knockout adult mice show reduced newborn neurons in the OB yet no defect of embryonic neurogenesis[15]. Thus, Thbs4 is an important regulator of adult neurogenesis hypothesized to facilitate neuroblast migration in the RMS[15]. Interestingly, Otx2 influences PNN formation in the visual cortex[20,25] and has been shown to control expression of extracellular glycoproteins and glycosaminoglycans *in vitro*, including Tnc[26,27]. In addition, *Otx2* knockdown in the mouse retina leads to reduced *Thbs4* expression[28] and an Otx2-binding element has been recently identified in the *Thbs4* gene[29]. However, while *Tnc* knockout mice show no signs of altered adult neurogenesis[22], we observe increase Tnc expression in mice showing decreased neurogenesis. We find increased *Thbs4* expression results in decreased neurogenesis, contrary to what might be expected given the results with *Thbs4* knockout mice. Also, while Thbs4 parallels Otx2 expression in the retina, we find increased Thbs4 expression in aSVZ after Otx2 knockdown. Nevertheless, changes in aSVZ expression of *Tnc* and *Thbs4* upon Otx2 knockdown are in-keeping with a transcriptional role for Otx2 in astrocytes.

Since we observe changes in neurogenesis that do not go along with results with Tnc and Thbs4 knockout mice, we cannot exclude that other targets of Otx2 being modified in aSVZ and RMS astrocytes upon sequestering of Otx2 in CSF. While large-scale mRNA sequencing analysis might reveal further astrocytic transcription targets of Otx2, we must keep in mind that Otx2 also regulates translation[25,30]. Although we do not know to what extent, ECM molecules are clearly altered by the loss of Otx2, suggesting that ECM composition must be tightly controlled to maintain proper neurogenesis. While a ~20% decrease in OB newborn neurons occurred after *Otx2* knockdown, and no change in aSVZ proliferation was observed, we find that Otx2 can influence neuroblast migration *in vitro*.

Taken together, non-cell-autonomous Otx2 might regulate neurogenesis though astrocyte-derived ECM control of neuroblast migration.

Interestingly, homeoproteins have been previously implicated as molecular clues for axon guidance and cell migration. Extracellular gradients of either Otx2 or Engrailed were able to guide growth cones of frog retinotectal axons *in vitro* through internalization and regulation of local translation[31]. Furthermore, abnormal routing of retinotectal axons was observed *in vivo* in the developing chick tectum upon expression of anti-Engrailed scFv to neutralize extracellular Engrailed[32]. In the developing chick ventral neural tube, the Pax6 homeoprotein was found to influence the migration of oligodendrocyte precursor cells (OPC) through direct non-cell-autonomous activity[33]. Although not necessarily implicated in OPC migration, *Tnc* expression patterns and isoforms in the embryonic mouse brain were found to be regulated by Pax6[34]. Consistent with these observations, CSF-derived Otx2 reveals a role for homeoprotein non-cell-autonomous regulation of cell migration in the adult brain.

Methods

Mice and ethics statement

S129 mice were purchased from Charles River Laboratories. Otx2-lox mice were kindly donated by Dr. T. Lamonerie[35] and *Otx2*$^{+/GFP}$ mice were kindly donated by Dr. A. Simeone[36]. scFv-Otx2 knock-in mouse lines were previously described[14]. All animal procedures, including housing, were carried out in accordance with the recommendations of the European Economic Community (86/609/EEC), the French National Committee (87/848) and French bylaws (AGRG1240332A / AGRG1238724A / AGRG1238767A / AGRG1238729A / AGRG1238753A). For surgical procedures, animals were anesthetized with Xylazine (Rompun 2%, 5 mg/kg) and Ketamine (Imalgene 500, 80 mg/kg). For biochemical analysis, mice were sacrificed by cervical elongation. This research (project no. 00704.02) was approved by Ethics committee n° 59 of the French Ministry for Research and Higher Education. Mice were conventionally raised (12:12 hours light:dark cycle) in cages with red tunnels, nesting cotton, and with food and water ad libitum.

Mouse surgery

Cre-Tat recombinant protein was produced as described[12]. Cre-Tat (8 to 20 µg/ml in 400 mM NaCl, 15% DMSO) or vehicle was injected as previously described[12]. 10 days after Cre-Tat injection, mice were injected intraperitonally with 150 mg/kg of BrdU (Sigma B9285 at 10 mg/ml diluted in NaCl 0.9%). For OB integration experiments, mice were injected twice daily for five days, and then housed for 3 weeks prior to perfusion with PBS. For proliferation experiments, mice were perfused with PBS two hours after one pulse of BrdU. Brains were cut in half: the anterior half was fixed for 48 h at 4 °C in 4% formaldehyde-PBS, immersed overnight in 20% sucrose PBS, and processed for cryostat sectioning; the posterior half was used to recover 4th ventricle choroid plexus for quantitative PCR analysis of *Otx2* expression.

Astrocyte cell culture

Primary astrocytes were prepared from cortex of newborn mouse (P0 to P4) and cultured in 10 mL of DMEM high glucose, 10% serum, 1x antimitotic/antibiotic. After 7 days, astrocytes were passaged into 6-well plates at 400 000 cells/ml for RNA/protein analysis, and into 24-well plates at 100 000 cells/ml with coverslips for immunohistochemistry. For protein treatments, passaged astrocytes were incubated 14 days and then were treated with 1% Ara-C (in DMEM high glucose, 1% B27, 1x antimitotic/antibiotic) for 24h prior to treatment with 100 ng/ml Otx2 protein. After 24h, astrocytes were either processed for analysis or used for neurosphere co-culture. For transfections, passaged astrocytes were grown to 80% confluency

and then transfected by using either lipofectamine for plasmids or oligofectamine for siRNA. After 3 days, astrocytes were either processed for analysis or used for neurosphere co-culture.

Adult neurosphere cell culture

Neurosphere cultures were prepared from 3-month-old mouse SVZ and grown in 1 mL of DMEM/F12 2% B27 20 ng/ml EGF 10 ng/mL bFGF 1x antimitotic/antibiotic per well in a 24 well-plate for 10 days according to standard protocols[37]. Free-floating neurospheres were passaged by dissociation with acutase. After 4 days, passaged neurospheres were individually transferred onto astrocytes prepared for co-culture. After 3 days, co-cultures were washed with PBS and were either process for RNA/protein analysis or were fixed 15 min with 4% formaldehyde-PBS for immunohistochemistry.

Immunohistochemistry and histology

Frozen brains were sectioned (25 µm) by cryostat and stored at -20 °C. Slides were thawed 15 min at room temperature, hydrated in PBS, and incubated in a steamer for 15 min with 10 mM citrate buffer, pH 6. After cooling, sections were washed with PBS and incubated in blocking buffer (0.5% Triton-X, 10% normal donkey serum (Abcam) in PBS) for 30 min. Primary antibodies were incubated overnight at room temperature (anti-BrdU OBT0030 ABD Serotech 1/100; anti-Otx2 ab92326 Abcam 1/250; anti-DCX AB2253 Millipore 1/1000; anti-GFAP G6171 Sigma 1/200; anti-Vimentin AB5733 Millipore 1/1000; anti-GFP ab13970 Abcam 1/1000). After PBS washes, secondary antibodies were incubated 2 hours at room temperature (Donkey anti-IgG Alexa fluor antibody Invitrogen 1/2000 or anti-guinea pig biotinylated ab6907 Abcam 1/500). Sections treated with biotinylated secondary antibodies were further incubated 2 hours with dye-conjugated streptavidin (Invitrogen). Sections were dried and mounted in Dapi Fluoromount-G. Imaging was performed with an inverted confocal microscope (Leica), a Nikon 90i upright widefield, or a Spinning-disk with constant parameters. For BrdU analysis, one section every 200 µm was quantified. Counting was performed using ImageJ software with systematic methods (background correction and thresholding). In situ hybridization was performed as previously described[12].

Quantitative PCR

Total RNA from 4th ventricle choroid plexus was extracted with the RNeasy Lipid Tissue Mini Kit (Qiagen) with DNA removal. RNA and protein were extracted for ECM composition analysis using the AllPrep DNA/RNA/Protein Mini Kit (Qiagen). RNA was processed with the QuantiTect Reverse Transcription Kit (Qiagen). cDNA was diluted 1/10 with RNase-free water for quantitative PCR, samples, which were analyzed in triplicate with a LightCycler 480 II (Roche) and SYBR Green I Master mix. After T_m profile validation, gene-to-HPRT ratios were determined by the $2^{-\Delta\Delta Ct}$ method. For *Otx2* expression analysis, mean expression of vehicle-injected mice was used for comparison.

RMS microdissection

Brain was placed in cold PBS, dorsal side facing up, and two equidistant longitudinal incisions in each OB were made to divide them in 3 parts while keeping them attached to the rest of the brain. The aSVZ was then microdissected as previously described[38]. Afterwards, the hemispheres were placed once again dorsal side facing up and the sagittal cuts starting from the OB incisions were pursued the entire length of the brain. The central piece of tissue was laid on its side and RMS was cut out, as shown in Fig. 2d.

Immunoprecipitation and Western blot

Tissue was microdissected and stored at -80 °C. Tissues were triturated in 100 µl of lysis buffer (150 mM NaCl, 1% Triton, 100 mM Tris, pH 7.4, 10 mM EDTA, 1X protease/phosphatase inhibitor (Roche)) per 10 mg of tissue and incubated 10 min on ice. Supernatant was recovered in low binding tubes after centrifugation for 10 min at 16 000*g*. Antibody was added (2.5 ug of anti-Otx2 (ab21990, Abcam) or anti-IgG (ab27478, Abcam) and incubated overnight at 4 °C with rotation. Protein A sepharose beads (GE Healthcare) were washed twice and resuspended 1:1 with lysis buffer. Beads (30 µl) were added to each sample and incubated 3 h at 4 °C. Beads were recovered by centrifugation for 1 min at 16 000*g* and washed 5 times with 1 mL of cold wash buffer (Lysis buffer with 500 mM NaCl). Proteins were eluted from the beads with 30 µl of 2X laemmli buffer, heated 5 min at 95 °C, and stored at -20 °C.

Samples were separated on NuPage 4-12% Bis-Tris precasted gels (Invitrogen) with 1X MES buffer and antioxidant (Invitrogen), then processed for Western Blotting for Otx2 detection. Membranes were blocked in 5% non-fat milk, TBS, 0.2% Tween, incubated with anti-Otx2 (in-house mouse monoclonal) overnight at 4 °C, washed, and then incubated with anti-mouse HRP-conjugated (GeneTex) for 2 h at room temperature. Chemiluminescence reaction was performed with ECL femto (Thermo Scientific).

Statistical analysis

Prism 6 software (GraphPad) was used for all statistical analysis. Sample size was determined after preliminary experiments. Quantification was normalized by the mean value of vehicle-injected mice samples. Normal data distribution was assessed by the D'Agostino & Pearson omnibus normality test, except for Fig. 5c,d where the Shapiro-Wilk test was used due to reduced n. If normal test was not passed, Mann-Witney was applied; otherwise, unpaired t-test with Welch's correction was used (noted t-test in Legends). See Figure Legends for relevant statistical tests.

Acknowledgements

This work was supported by Région Ile-de-France via le DIM Cerveau et Pensée, by ERC Advanced Grant HOMEOSIGN n°339379, and by GRL Program n°2009-00424.

Author Contributions

APl, VOM, APr and AAD designed the experiments; APl, VOM and CD performed the experiments; APl, VOM and AAD wrote the manuscript.

References

1. Lledo, P.-M. & Valley, M. *Cold Spring Harb Perspect Biol* **8**, (2016).
2. Lois, C., García-Verdugo, J.M. & Alvarez-Buylla, A. *Science* **271**, 978–981 (1996).
3. Whitman, M.C., Fan, W., Rela, L., Rodriguez-Gil, D.J. & Greer, C.A. *J Comp Neurol* **516**, 94–104 (2009).
4. Kaneko, N. et al. *Neuron* **67**, 213–223 (2010).
5. Shen, Q. et al. *Cell Stem Cell* **3**, 289–300 (2008).
6. Silva-Vargas, V., Maldonado-Soto, A.R., Mizrak, D., Codega, P. & Doetsch, F. *Cell Stem Cell* **19**, 643–652 (2016).
7. Bjornsson, C.S., Apostolopoulou, M., Tian, Y. & Temple, S. *Dev Cell* **32**, 435–446 (2015).
8. Lehtinen, M.K. et al. *Journal of Neuroscience* **33**, 17553–17559 (2013).
9. Sawamoto, K. et al. *Science* **311**, 629–632 (2006).
10. Prochiantz, A. & Di Nardo, A.A. *Neuron* **85**, 911–925 (2015).
11. Curto, G.G. et al. *Stem Cells Dev.* **23**, 2813–2830 (2014).

12. Spatazza, J. et al. *Cell Rep* **3**, 1815–1823 (2013).
13. Hoch, R.V., Lindtner, S., Price, J.D. & Rubenstein, J.L.R. *Cell Rep* **12**, 482–494 (2015).
14. Bernard, C. et al. *PLoS Genet* **12**, e1006035 (2016).
15. Girard, F., Eichenberger, S. & Celio, M.R. *Mol Cell Neurosci* **61**, 176–186 (2014).
16. Jankovski, A. & Sotelo, C. *J Comp Neurol* **371**, 376–396 (1996).
17. Sugiyama, S. et al. *Cell* **134**, 508–520 (2008).
18. Lee, H.H.C. et al. *Mol Psychiatry* **22**, 680–688 (2017).
19. Beurdeley, M. et al. *Journal of Neuroscience* **32**, 9429–9437 (2012).
20. Bernard, C. & Prochiantz, A. *Neural Plast.* **2016**, 1–7 (2016).
21. Dityatev, A., Seidenbecher, C.I. & Schachner, M. *Trends Neurosci* **33**, 503–512 (2010).
22. Kazanis, I., Belhadi, A., Faissner, A. & Ffrench-Constant, C. *Journal of Neuroscience* **27**, 13991–13996 (2007).
23. Benner, E.J. et al. *Nature* **497**, 369–373 (2013).
24. Wiese, S., Karus, M. & Faissner, A. *Front Pharmacol* **3**, 120 (2012).
25. Hou, X. et al. *Sci Rep* **7**, 12646 (2017).
26. Gherzi, R. et al. *DNA Cell Biol.* **16**, 559–567 (1997).
27. Nguyen Ba-Charvet, K.T., Boxberg, von, Y., Guazzi, S., Boncinelli, E. & Godement, P. *Development* **125**, 4273–4282 (1998).
28. Housset, M. et al. *Journal of Neuroscience* **33**, 9890–9904 (2013).
29. Peña, C.J. et al. *Science* **356**, 1185–1188 (2017).
30. Nedelec, S. et al. *Proc Natl Acad Sci USA* **101**, 10815–10820 (2004).
31. Brunet, I. et al. *Nature* **438**, 94–98 (2005).
32. Wizenmann, A. et al. *Neuron* **64**, 355–366 (2009).
33. Di Lullo, E. et al. *Development* **138**, 4991–5001 (2011).
34. Holst, von, A., Egbers, U., Prochiantz, A. & Faissner, A. *J Biol Chem* **282**, 9172–9181 (2007).
35. Fossat, N., Chatelain, G., Brun, G. & Lamonerie, T. *EMBO Rep* **7**, 824–830 (2006).
36. Acampora, D., Di Giovannantonio, L.G., Di Salvio, M., Mancuso, P. & Simeone, A. *Mech Dev* **126**, 882–897 (2009).
37. Ferrón, S.R. et al. *Nature protocols* **2**, 849–859 (2007).
38. Mirzadeh, Z., Doetsch, F., Sawamoto, K., Wichterle, H. & Alvarez-Buylla, A. *J Vis Exp* (2010).doi:10.3791/1938

Figure Legends

Figure 1. Otx2 knockdown in the choroid plexus reduces newborn neurons in the olfactory bulb. (**a-c**) Conditional *Otx2* knockdown paradigm with Otx2-lox mice. (**a**) Staining for Otx2 in lateral ventricle choroid plexus 35 d after intracerebroventricular (icv) injection of vehicle or Cre-Tat. Scale bar, 200 µm. (**b**) Quantitative PCR analysis of *Otx2* expression in 4th ventricle (****P<0.0001, Mann-Whitney test, 5 experiments). (**c**) Comparison of *Otx2* expression levels between lateral and 4th ventricles from the same brain after Cre-Tat icv injection. (**d**) Schematic of adult (3 months) neurogenesis paradigm. (**e**) Staining for BrdU in olfactory bulbs 3 weeks post-injection. Scale bar, 400 µm. (**f**) Quantification of BrdU-positive cells in granule cell layer (GCL) (***P<0.001, t-test, 3 experiments). (**g**) Quantification of BrdU-positive cells in glomerular layer (GL) (*ns*=P>0.05, t-test, 3 experiments). (**h**) Staining for caspase and Dcx in RMS. Scale bar, 100 µm. (**i**) Quantification of caspase/Dcx co-labeled cells in RMS (*ns*=P>0.05, Mann-Whitney test, 3 experiments, error bars represent s.d.). (**j**) Schematic of adult (3 months) aSVZ proliferation paradigm. (**k**) Staining for BrdU in aSVZ 2 hours post-injection. Scale bar, 200 µm. (**l**) Quantification of BrdU-positive cells in aSVZ (*ns*=P>0.05, t-test, 2 experiments).

Figure 2. Otx2 in RMS and aSVZ is non-cell-autonomous. (**a-c**) Absence of *Otx2* expression in aSVZ (in **a** and **c**) and RMS (in **b**) as shown by GFP staining in *Otx2*$^{+/GFP}$ mice (in **a** and **b**) and *in situ* hybridization (in **c**). Note the expression of GFP in choroid plexus in **a**. Scale bars, 100 µm in **a** and **b**, 250 µm in **c**. (**d**) RMS microdissection on sagittal section. Scale bar, 1 mm. (**e**) Western blot analysis of Otx2 immunoprecipitation from lysate of various brain regions. Bands include Otx2 (<40 kDa), IgG (25 and 55 kDa), and unknown (~45 kDa). SC, superior colliculus; Str, striatum. (**f-h**) Staining for Otx2, Dcx, GFAP and Dapi in sagittal sections showing the aSVZ (in **f** and **h1-2**), RMS (in **f**, **g**, and **h3-5**) and OB (in **g** and **h6**). Boxes 1-6 in **f** and **g** are magnified in **h.** Scale bars, 300 µm in **f** and **g**, 100 µm in **h**.

Figure 3. Non-cell-autonomous Otx2 is sufficient to regulate adult neurogenesis. (**a**) Efficient recombination in choroid plexus of scFv-Otx2 mice after icv injection of Cre-Tat assessed by GFP reporter. Scale bar, 200 µm. (**b**) Quantification of BrdU-positive cells in granule cell layer (GCL) to assess adult neurogenesis (paradigm in Fig. 1d) in scFv-Otx2 mice. (**c**) Quantification of BrdU-positive cells in glomerular layer (GL) (*ns* = P>0.05, **P< 0.01, t-test, 3 experiments, error bars represent s.d.).

Figure 4. Otx2 transfers into supporting cells of neurogenic niches (**a**) In dorsal aSVZ, Otx2 staining is detected in GFAP-labeled astrocytes but not in Dcx-labeled neuroblasts. Scale bar, 100 µm. Arrows highlight astrocytes containing Otx2. (**b**) Along the lateral ventricular wall, Otx2 staining is detected in vimentin (Vim) labeled ependymal cells. Scale bar, 30 µm. (**c**) In the RMS, Otx2 staining is detected in GFAP-labeled astrocytes but not in Dcx-labeled neuroblasts. Scale bar, 30 µm. Arrows highlight astrocytes containing Otx2. (**d**) Orthogonal projection shows Otx2 in the nucleus of astrocytes within the RMS.

Figure 5. Otx2 regulates expression of ECM proteins to impact neuroblast migration. (**a-d**) Quantitative PCR analysis of *Thbs4* (**a, c**) and *Tnc* (**b, d**) expression in aSVZ of Otx2-lox mice (**a, b**) or scFv-Otx2 mice (**c, d**) after icv injection of Cre-Tat or vehicle (*P< 0.05, **P< 0.01, ***P< 0.001, ****P< 0.0001, t-test, 3 experiments). (**e**) Schematic of *in vitro* neurogenesis paradigm. (**f**) Quantitative PCR analysis of *Tnc* expression in Otx2-treated astrocytes (**P< 0.01, t-test, 3 experiments). (**g-h**) Staining of astrocytes (GFAP, green),

neuroblast (Dcx, red) and nucleus (Dapi, blue) on astrocyte-plated neurospheres treated without (**g**) or with Otx2 protein (**h**). (**i**) Number of neuroblasts migrating out from neurospheres onto astrocytes treated or not with Otx2 protein (*P< 0.05, t-test, 2 experiments). Error bars represent s.d.

Figure 1

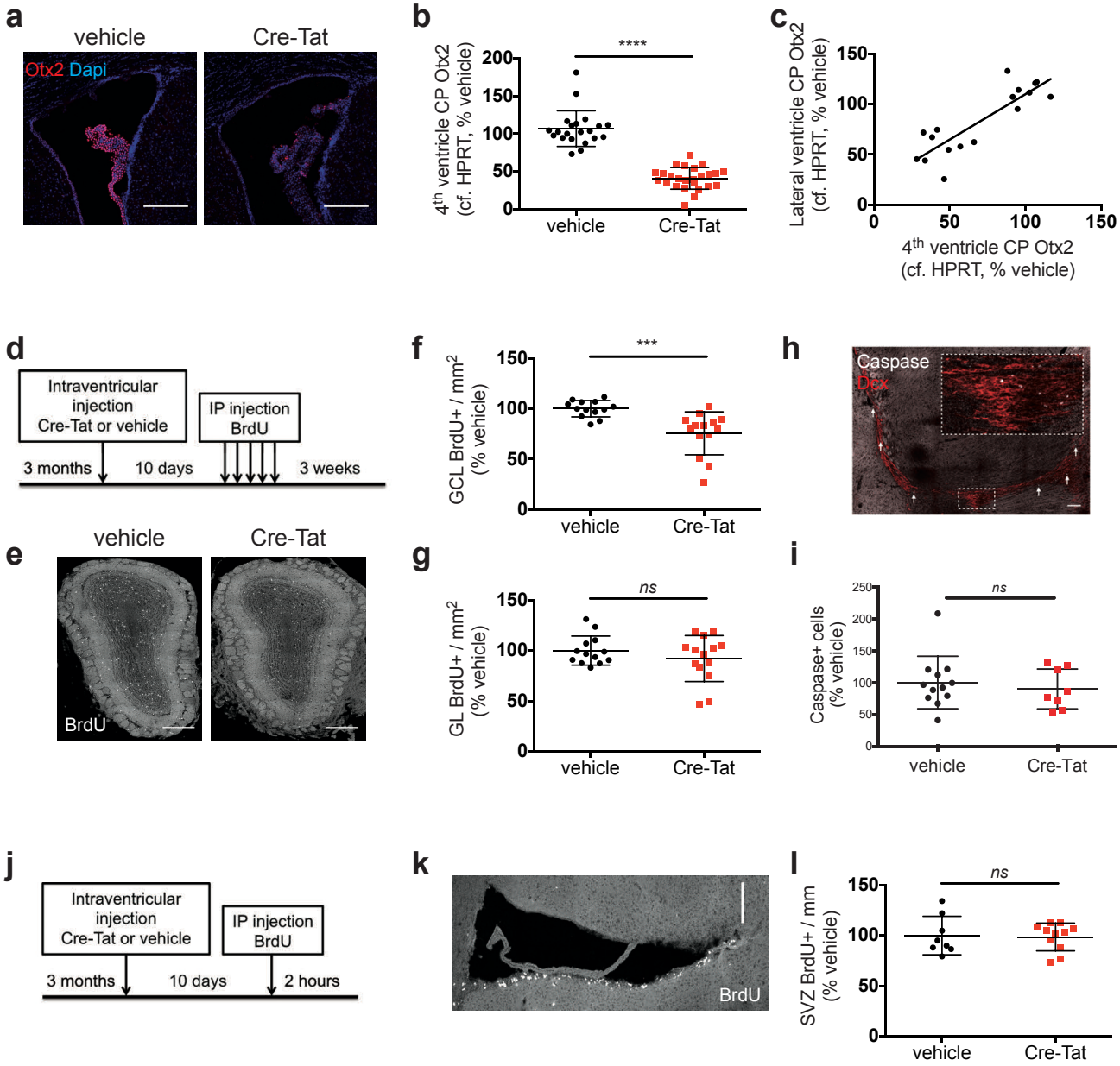
a
vehicle
Cre-Tat
Otx2 Dapi
b
4th ventricle CP Otx2 (cf. HPRT, % vehicle)
****
vehicle
Cre-Tat
c
Lateral ventricle CP Otx2 (cf. HPRT, % vehicle)
4th ventricle CP Otx2 (cf. HPRT, % vehicle)
d
Intraventricular injection Cre-Tat or vehicle
IP injection BrdU
3 months
10 days
3 weeks
e
vehicle
Cre-Tat
BrdU
f
GCL BrdU+ / mm2 (% vehicle)
***
vehicle
Cre-Tat
g
GL BrdU+ / mm2 (% vehicle)
ns
vehicle
Cre-Tat
h
Caspase
Dex
i
Caspase+ cells (% vehicle)
ns
vehicle
Cre-Tat
j
Intraventricular injection Cre-Tat or vehicle
IP injection BrdU
3 months
10 days
2 hours
k
BrdU
l
SVZ BrdU+ / mm (% vehicle)
ns
vehicle
Cre-Tat

Figure 2

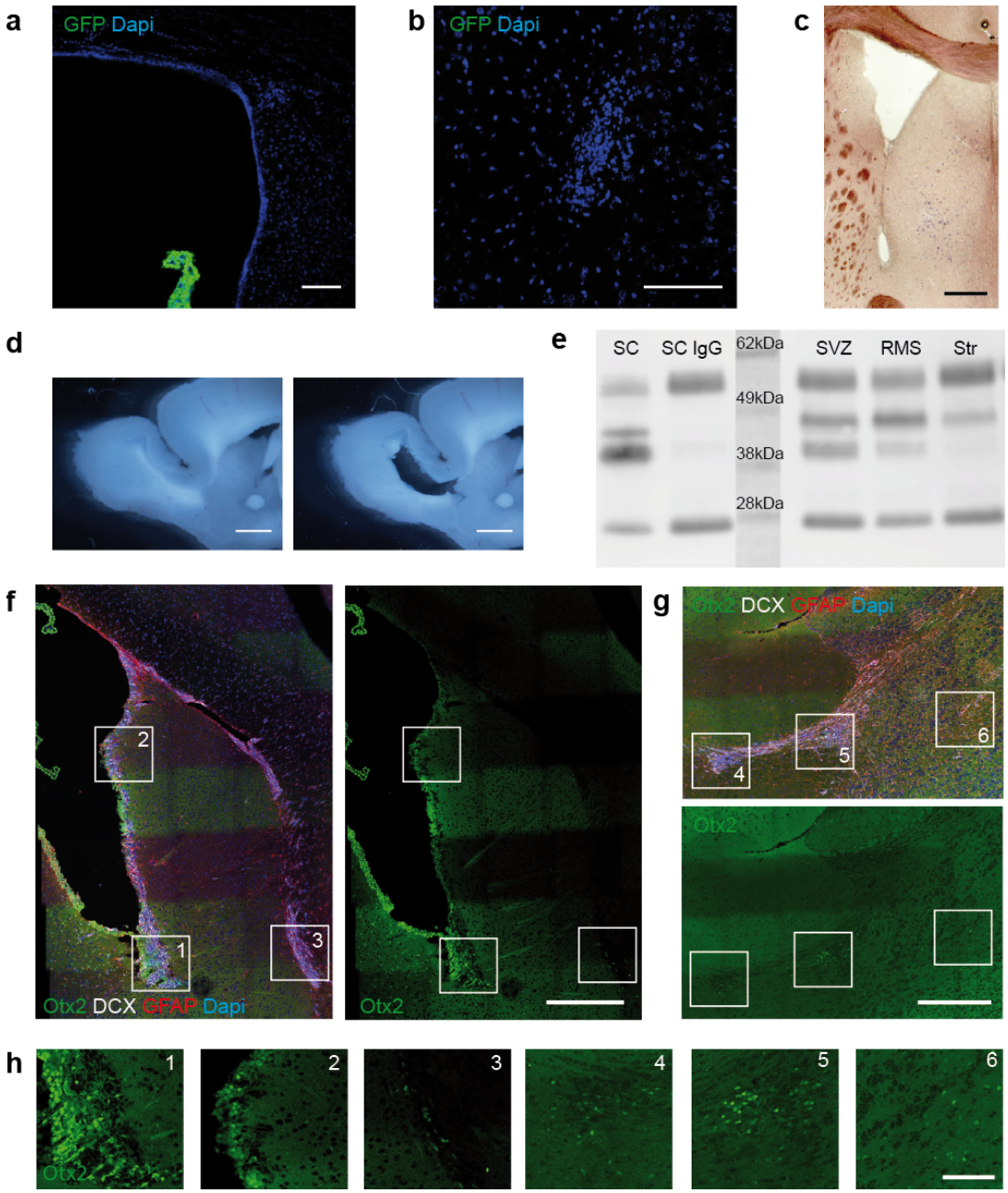
a
GFP Dapi
b
GFP Dapi
c
d
e
SC
SC IgG
62kDa
49kDa
38kDa
28kDa
SVZ
RMS
Str
f
2
1
3
Otx2 DCX GFAP Dapi
Otx2
g
Otx2 DCX GFAP Dapi
4
5
6
Otx2
h
1
2
3
4
5
6
Otx2

Figure 3

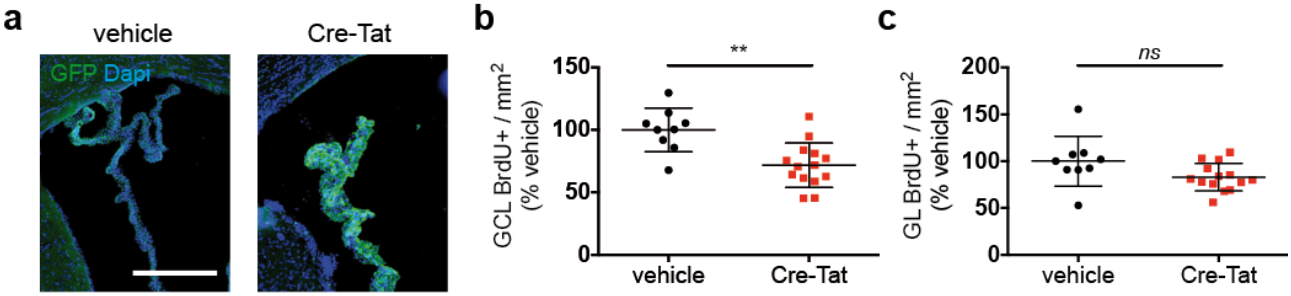
a
vehicle
Cre-Tat
GFP Dapi
b
GCL BrdU+ / mm2
(% vehicle)
150
100
50
0
**
vehicle
Cre-Tat
c
GL BrdU+ / mm2
(% vehicle)
200
150
100
50
0
ns
vehicle
Cre-Tat

Figure 4

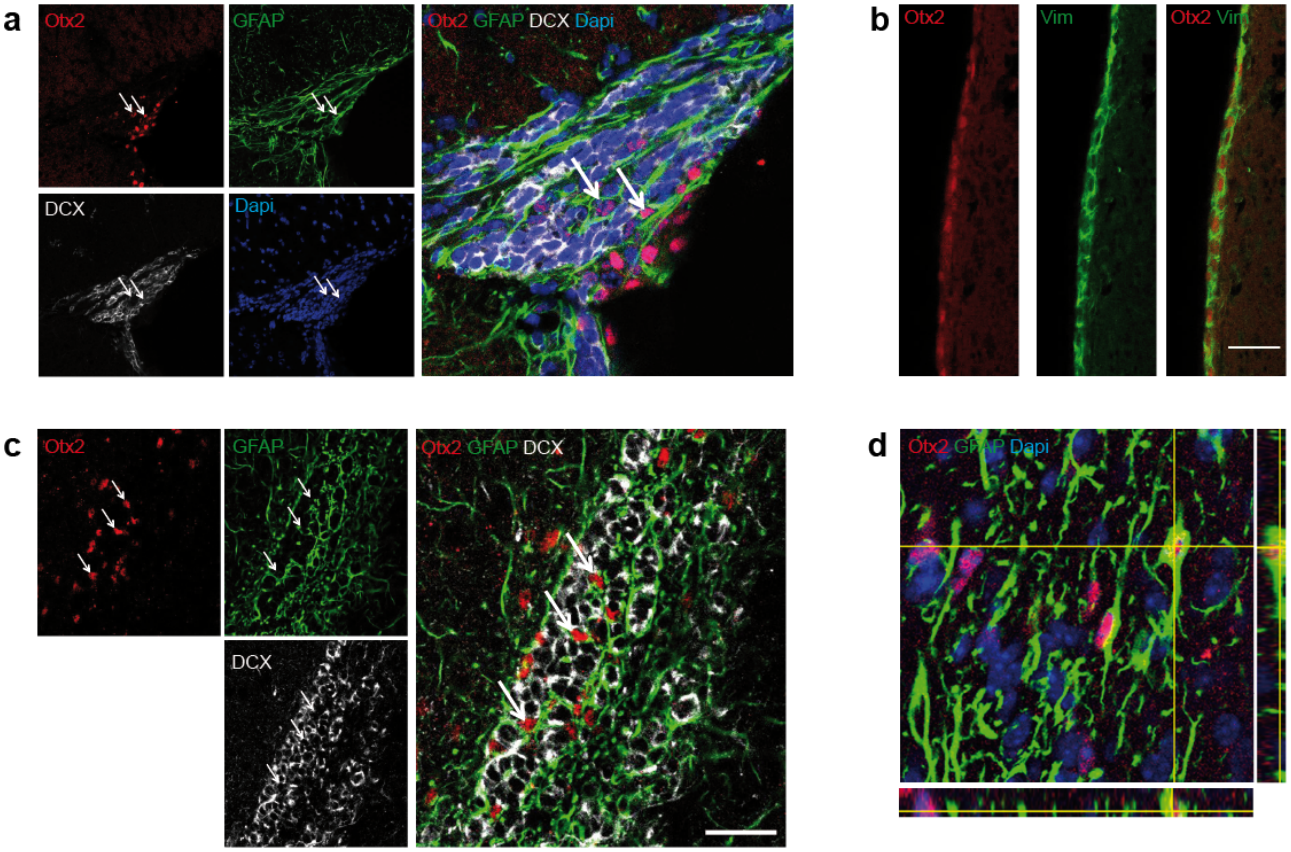
a
Otx2
GFAP
Otx2 GFAP DCX Dapi
DCX
Dapi
b
Otx2
Vim
Otx2 Vim
c
Otx2
GFAP
Otx2 GFAP DCX
DCX
d
Otx2 GFAP Dapi

Figure 5

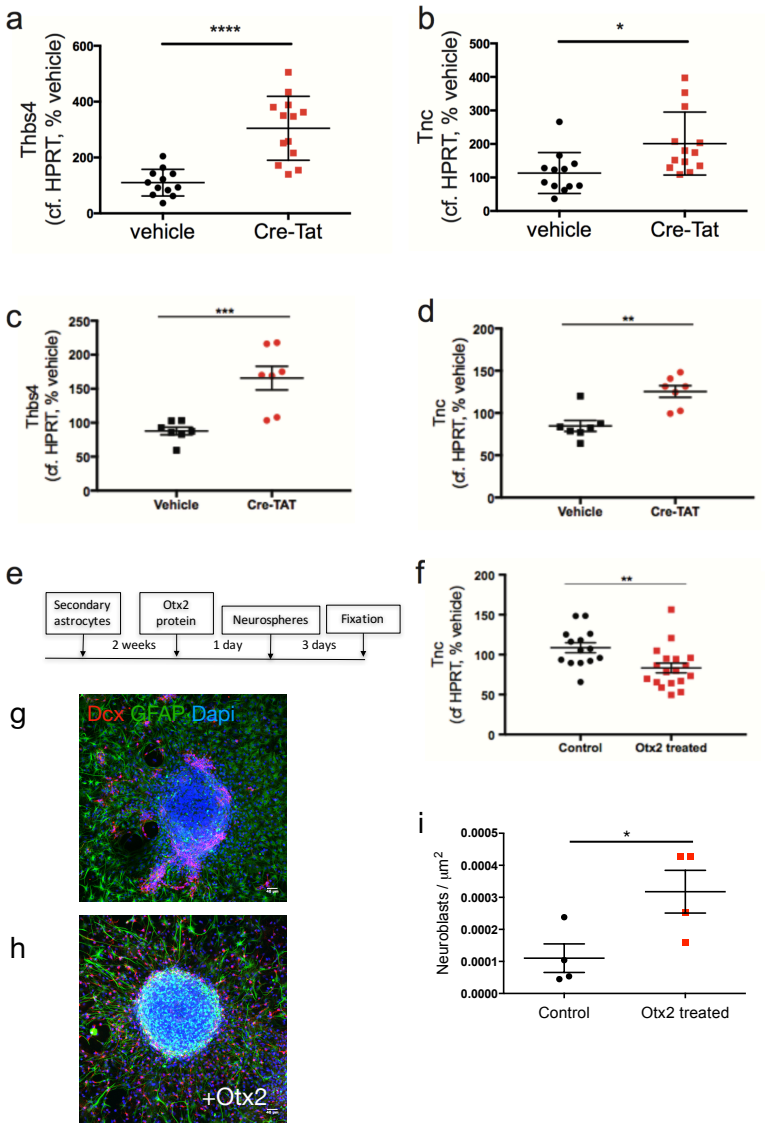
a
Thbs4
(cf. HPRT, % vehicle)
****
vehicle
Cre-Tat
b
Tnc
(cf. HPRT, % vehicle)
*
vehicle
Cre-Tat
c
Thbs4
(cf. HPRT, % vehicle)
***
Vehicle
Cre-TAT
d
Tnc
(cf. HPRT, % vehicle)
**
Vehicle
Cre-TAT
e
Secondary astrocytes
Otx2 protein
Neurospheres
Fixation
2 weeks
1 day
3 days
f
Tnc
(cf HPRT, % vehicle)
**
Control
Otx2 treated
g
Dcx GFAP Dapi
h
+Otx2
i
Neuroblasts / µm2
*
Control
Otx2 treated